Gamma-ray multipole mixing ratios in ^{71}Ge

W. D. Hamilton* and W. L. Croft
Mississippi State University, Mississippi State, Mississippi 39762

W. H. Brantley
Furman University, Greenville, South Carolina 29613

L. A. Rayburn and I. C. Girit†
Oak Ridge Associated Universities, Oak Ridge, Tennessee 38731

S. Brant and V. Paar
University of Zagreb, 41000 Zagreb, Republic of Croatia
(Received 1 March 1991)

The multipole mixing ratios of γ-ray transitions between low-lying states in ^{71}Ge were determined by measuring γ-ray anisotropies from oriented ^{71}As nuclei. Nuclear orientation of ^{71}As*Fe* samples occurred through the magnetic hyperfine interaction at 5 mK. The interacting boson-fermion model was used to calculate transition matrix elements and, in general, there is good agreement between experimental results and theoretical values of $E2$:$M1$ multipole mixing ratios.

PACS number(s): 23.20.Gq, 21.60.Ev, 23.20.En, 23.20.Js

I. INTRODUCTION

The structure of ^{71}Ge has recently been investigated both experimentally and theoretically [1]. Transitions following the β^+, electron capture (EC) decay of ^{71}As ($T_{1/2}=61$ h) were measured, and the theoretical analysis, within the framework of the interacting boson-fermion model [2–4], allowed branching ratios and the amplitudes of multipole mixing ratios to be determined. This analysis has been extended in the present report to interpret data obtained in measurements of the directional distribution of γ rays from oriented nuclei.

This technique was used in the past [5] to examine γ-ray transitions in ^{71}Ge and the present experiments confirm this earlier work and also extend the range of the measurements. The experiments demonstrate that useful off-line measurements may be made using the UNISOR dilution refrigerator with sources that are prepared during an on-line experiment. Thus, the effective operation of the facility and available beam time may be advantageously extended.

II. EXPERIMENTAL ASPECTS

A. Experimental method

The directional distribution of radiation from oriented nuclei is directly dependent on the multipolarity of the radiation and on the spins of the levels linked by the γ transition. The radiation distribution pattern is given by the equation

$$W(\theta)=1+a_2P_2(\cos\theta)+a_4P_4(\cos\theta)\ ,$$

where $a_\lambda=A_\lambda U_\lambda B_\lambda(I)Q_\lambda$. The A_λ coefficient describes the transition, with multipole components L and $L+1$, between initial and final states. The amplitude ratio $L+1$:L of these components is the mixing ratio δ whose sign corresponds to an emission process.[1] The orientation coefficient of the initial state, $B_\lambda(I)$, is given by

$$B_\lambda(I)=\sum_m(-1)^{I+m}[(2\lambda+1)(2I+1)]^{1/2}\times\begin{pmatrix} I & I & \lambda \\ -m & m & 0\end{pmatrix}g(m)\ ,$$

where $g(m)$ are the relative populations of the different magnetic substrates $|Im\rangle$ [cf. Ref. [6], Eq. (12.73)]. The $g(m)$ depend on the sample temperature and, in the case of the nuclear hyperfine interaction, on the magnetic-field strength that the nuclear magnetic moment experiences. The deorienting effect of transitions intermediate between the oriented state and the decaying level is contained in the U_λ coefficient:

$$U_\lambda(I_iI_fL)=(-1)^{I_i+I_f+\lambda+L}[(2I_i+1)(2I_f+1)]^{1/2}\times\begin{Bmatrix} I_i & I_i & \lambda \\ I_f & I_f & L\end{Bmatrix},$$

where I_i,I_f are the spins of the levels linked by a transition of angular momentum L [cf., Ref. [6], Eq. (12.210)]. The Q_λ term corrects for the finite size and efficiency of the detector [7].

*On leave from the University of Sussex, Sussex, England.
†Present address: Princeton University, Princeton, NJ 08544.

[1]This is the convention adopted by Nuclear Data Sheets.

The necessary low temperature is obtained with a ^{3}He:^{4}He dilution refrigerator. At the UNISOR facility the refrigerator is designed for on-line use but may also be operated in an off-line mode when baffles close the beam access to the cold finger. The off-line mode has the great advantage that the base temperature, when the contribution from source heating is very low, is ~ 5 mK. Thus, under favorable circumstances a high degree of orientation may be achieved.

The design of the refrigerator allows a sample to be top loaded without disturbing the operating conditions. It is thus possible to achieve close to the base temperature several hours after loading. Cooling after this time is at a very low rate and, if the degree of orientation is already close to saturation, no significant changes occur.

Detectors are placed around the sample in a plane containing the magnetic-field direction. Altogether up to eight detectors at 45° separations may be used with two detectors placed along the axis of the field and two perpendicular to this axis. The high degree of symmetry, although important in on-line measurements, has no particular significance in off-line experiments, while the large number of detectors allows several separate measurements to be made simultaneously.

B. Source preparation

Sources were prepared by bombarding natural and enriched (95% ^{63}Cu) copper foils with ^{12}C. The ^{63}Cu foil of 2.3 mg cm^{-2} was bombarded for 2.25 h with a 55-MeV, 450-nA beam (charge state 6^+) and a natural copper foil of 4.5 mg cm^{-2} was bombarded for 5.75 h with a 165-MeV, 500-nA beam. The irradiations conditions were set by on-line measurements and, while these were satisfactory for the range of isotopes of interest that were produced in the enriched target, degrading foils were placed before the natural target foil to reduce the beam energy. The target foils were backed by several thin 3.19-mg cm^{-2} foils of pure iron. Reaction products were caught in this stack and the foil containing the maximum activity of interest was easily identified. The number of reaction products was small and, since the decay schemes of the longer-lived isotopes are mostly simple, the variety of activities posed no problem.

This method of source preparation had the great advantage that the activities were implanted directly into, and approximately uniformly throughout, the foils. Foils from the two irradiations were used. In the first measurement, an unannealed foil was soldered with Wood's metal to the end of the cold finger of the refrigerator. A second experiment was made with a foil that had been annealed for 6 h at 840 °C in a stream of flowing hydrogen. In each case a ^{57}Co*Fe* thermometer was soldered on top of the source foil and this indicated the maximum temperature of the source.

Measurements were delayed until 4 days after source preparation, and all short-lived activities had decay to negligible levels.

C. Data collection

Spectra from the detectors were collected for 1-h periods when the sample was cold (~ 5 mK) and warm (~ 1 K). Temperature cycling occurred every 10 h and the data corresponding to the first hour of cooling was rejected from the analysis. The consistency of data collected after this initial hour indicated that further cooling had an insignificant effect on count rate changes. This is consistent with the $B_2(I)$ coefficient being close to its saturation value when the temperature approaches 5 mK so that the small subsequent fall in temperature caused no detectable count rate change. The electronic stability against gain shift was sufficiently good and temperature changes so small that the individual 1-h spectra could be summed for each sample temperature. The anisotropies of the dominant peaks were obtained from the integrated peak counts recorded in the detectors on the axis and perpendicular to the axis. The anisotropies are defined by the ratios

$$\mathcal{A}_0 = 1 - W(0) = -A_2 B_2(I) U_2 Q_2 - A_4 B_4(I) U_4 Q_4 ,$$

$$\mathcal{A}_{\pi/2} = W(\pi/2) - 1 = \tfrac{1}{2}[A_2 B_2(I) U_2 Q_2] - \tfrac{3}{8}[A_4 B_4(I) U_4 Q_4] .$$

The spectra contained contributions from isotopes of different half-lives, and half-life corrections were applied to permit the anisotropies to be obtained from the sequence of measurements. These contributions were identified initially by the γ-ray transition energies from expected reaction products and were confirmed by following their decays during the course of the measurement. Only data taken when the sample was warm, and the orientation random, were used in this test. The same procedure was followed for the annealed source.

We found that the sets of anisotropies for the two sources were entirely consistent and equal to within 3% indicating that the annealing of the second sample produced no noticeable improvement. However, it cannot be concluded that annealing of the thin sample foil was unnecessary. To an extent, which we cannot determine with any certainty, we know that annealing took place at the time of source production. This was a direct result of the heating produced in the stacked foils when the beam was stopped in them. This occurred in vacuum throughout the time of source production and subsequently the foils, together with their holder, took about 20 min to reach room temperature. Thus, further lengthy annealing appears unnecessary and this has an important time-saving advantage when short-lived activities are produced in this way. However, it should be noted that there is little control on foil temperature or on the temperature distribution throughout the foil.

D. Data analysis

Transitions belonging to the ^{71}As decay and also to the decays of ^{74}As to ^{74}Se and ^{74}Ge were analyzed. The latter decays are both well understood and occur almost exclusively to the ground states or the first excited 2^+ levels. Now the spin of ^{74}As is 2^- and thus the anisotropy of the 2^+-0^+ transitions are uniquely determined since we may expect the $2^-(\beta)2^+$ transition to be first forbidden $\Delta j_\beta = 0$ with deorientation coefficients $U_\lambda = 1$. The

analysis of the anisotropies of the 2^+-0^+ γ rays in ^{74}Se and ^{74} Ge gave identical results (Table I), and showed that we had obtained the maximum effect consistent with the temperature of the measurements (5.1 ± 0.1 mK), the magnetic moment of ^{74}As [$\mu=-1.597(3)\mu_N$], and the internal field that it experiences in iron [$B_{\rm hf}=34.39(3)$ T]. Thus, all ^{74}As nuclei experience maximum orientation and we may expect the same to be true for ^{71}As. These maxima occur for $B_2(I)$ values close to their saturation values; this is true for both ^{71}As and ^{74}As as their magnetic moments have comparable magnitudes. Close to saturation a $B_\lambda(I)$ value is insensitive to small temperature changes and it is this feature that permitted the data obtained in the "cold" runs to be summed.

There is little doubt about spin assignments to levels in ^{71}Ge [1] and in several cases the present results provide unambiguous values. Only second-order terms were useful in the ^{71}Ge analysis as the $B_4(I)$ value is small and thus a_4 coefficients are also small but with comparatively large errors.

E. Evaluation of $B_\lambda(I)$ coefficients

There is an excellent consistency between the $B_\lambda(I)$ values obtained from the anisotropies of the 595- (^{74}Ge) and 634-keV (^{74}Ga) transitions. Our calculated values for a temperature of 5 mK give $B_2=0.944$ [B_2(sat)$=1.195$] and $B_4=0.129$ [B_4(sat)$=0.267$]. While there is good agreement between measured and calculated values of the second-order term, it is apparent that the calculated fourth-order coefficient is significantly smaller than that evaluated from the measured anisotropies and the known A_λ and U_λ coefficients. This could arise from a small admixture of higher angular momentum components in the β transition; this will have a much greater influence on U_4 since the higher components contribute negative values. However, it is not important in the present analysis which relies on second-order terms.

With $\mu(^{71}\text{As})=1.674(2)_\lambda$ and $I^\pi=\frac{5}{2}^-$ [15] we deduce that $B_2=1.01$ [B_2(sat)$=1.336$]. This is sufficiently close to the saturation value to make it insensitive to small

TABLE I. Measured γ-ray anisotropies of transitions in ^{71}Ge, ^{74}Ge, and ^{74}Se, and the U_2A_2 coefficients for ^{71}Ge.

E(level) (keV)	E(δ-ray) (keV)	I_i	I_f	$a_2(\Delta a_2)$	$a_4(\Delta a_4)$	U_2A_2	U_2A_2 Ref. [5]
				71 germanium			
175	175	$\frac{5}{2}^-$	$\frac{1}{2}^-$	−0.322(9)	0.008(10)	−0.303(9)	−0.330(2)
500	500	$\frac{3}{2}^-$	$\frac{1}{2}^-$	0.221(18)	−0.018(21)	0.208(17)	0.227(10)
525	350	$\frac{5}{2}^+$	$\frac{5}{2}^-$	−0.20(26)	−0.22(31)	−0.19(25)	
	327		$\frac{9}{2}^+$	−0.178(21)	−0.014(25)	−0.165(20)	−0.155(9)
708	708	$\frac{3}{2}^-$	$\frac{1}{2}^-$	−0.16(17)	0.21(19)	−0.15(16)	
1026	1026	$\frac{5}{2}^-$	$\frac{1}{2}^-$	−0.45(16)	0.02(18)	−0.43(15)	−0.43(9)
	851		$\frac{5}{2}^-$	−0.43(29)	0.18(33)	−0.42(28)	
	526		$\frac{3}{2}^-$	0.69(5)	−0.04(6)	0.65(5)	0.65(3)
1095	1095	$\frac{3}{2}^-$	$\frac{1}{2}^-$	0.077(21)	−0.020(24)	0.072(20)	0.048(5)
	920		$\frac{5}{2}^-$	0.40(11)	−0.20(12)	0.38(10)	0.31(4)
1139	1139	$\frac{3}{2}^-$	$\frac{1}{2}^-$	−0.23(7)	−0.04(7)	−0.22(6)	−0.30(3)
	392		$\frac{5}{2}^-$	0.08(8)	−0.11(10)	0.08(8)	
1205	615	$\frac{5}{2}^+$	$\frac{7}{2}^+$	−0.17(9)	0.07(11)	−0.16(9)	
1212	1212	$\frac{5}{2}^-$	$\frac{1}{2}^-$	−0.21(18)	−0.14(21)	−0.20(17)	
	1037		$\frac{5}{2}^-$	−0.33(7)	−0.04(9)	−0.31(7)	
	712		$\frac{3}{2}^-$	0.75(16)	0.20(19)	0.70(15)	
1299	1299	$\frac{3}{2}^-$	$\frac{1}{2}^-$	0.22(24)	0.36(28)	0.21(23)	0.33(3)
1559	1033	$\frac{5}{2}^+$	$\frac{5}{2}^+$	−0.33(25)	0.11(29)	−0.31(24)	
				74 germanium			
596	596	2^+	0^+	−0.528(14)	−0.149(15)		
				74 selenium			
634	634	2^+	0^+	−0.501(37)	−0.149(40)		

TABLE II. Measured and calculated $E2{:}M1$ multipole mixing ratios of transitions in ^{71}Ge.

E(level) (keV)	$E(\gamma$ ray) (keV)	I_i	I_f	IBFM $B(E2)$ (e^2b^2)	IBFM $B(M1)$ (μ_N^2)	Expt. δ $(E2{:}M1)$	IBFM δ
1026	1026	$\frac{5}{2}_3^-$	$\frac{1}{2}_1^-$	0.0036		$E2$	∞
	851		$\frac{5}{2}_1^-$	0.0058	0.0014	$0.0^{+3.2}_{-0.26}$	-1.43
	526		$\frac{3}{2}_1^-$	0.0094	0.0268	-0.16 ± 0.03	-0.26
1095	1095	$\frac{3}{2}_4^-$	$\frac{1}{2}_1^-$	3×10^{-8}	2.10^{-7}	0.23 ± 0.02 or -3.2 ± 0.02	0.38
	920		$\frac{5}{2}_1^-$	6×10^{-7}	6.10^{-9}	0.36 ± 0.14 or $3.7\leq\delta\leq\infty$	-7.56
1139	1139	$\frac{3}{2}_5^-$	$\frac{1}{2}_1^-$	0.0136	0.00011	0.45 ± 0.05 or -6.8 ± 1.4	10.4
	392		$\frac{5}{2}_2^-$	0.0039	0.335	$0.06\leq\delta\leq0.09$ or $-(4.3^{+1.7}_{-1.1})$	-0.04
1205	615	$\frac{5}{2}_2^+$	$\frac{7}{2}_1^+$	0.022	0.290	$-(0.23^{+0.09}_{-0.08})$ or $-(2.6^{+0.7}_{-0.5})$	-0.14
1212	1212	$\frac{5}{2}^-$	$\frac{1}{2}^-$			$E2$	
	1037		$\frac{5}{2}^-$	Intruder state		-0.10 ± 0.06 or 2.1 ± 0.3	
	712		$\frac{3}{2}^-$			$-(0.19^{+0.11}_{-0.09})$ or $-(1.8^{+0.5}_{-0.4})$	
1299	1299	$\frac{3}{2}_6^-$	$\frac{1}{2}_1^-$	0.004	0.0074	0.04 ± 0.03 or -1.88 ± 0.11	0.80
1559	1033	$\frac{5}{2}_3^+$	$\frac{5}{2}_1^+$	6×10^{-5}	8.3×10^{-5}	$-0.26\leq\delta\leq3.0$	

temperature changes in the "cold" sets of measurements, after the initial cooling period.

Table I contains a listing of the product U_2A_2. Also included are the data obtained in a previous nuclear orientation experiment [5]. In general, there is good agreement between the results of the two measurements. In order to obtain the values of A_2 coefficients, it is necessary in several cases to make assumptions about the angular momentum Δj_β associated with the spin change that occurs in the β decay of the oriented initial state. This step in the analysis is the one that is open to reinterpretation. However, when there are several transitions from the same initial state, and one of these has known multipolarity and links states of established spin,

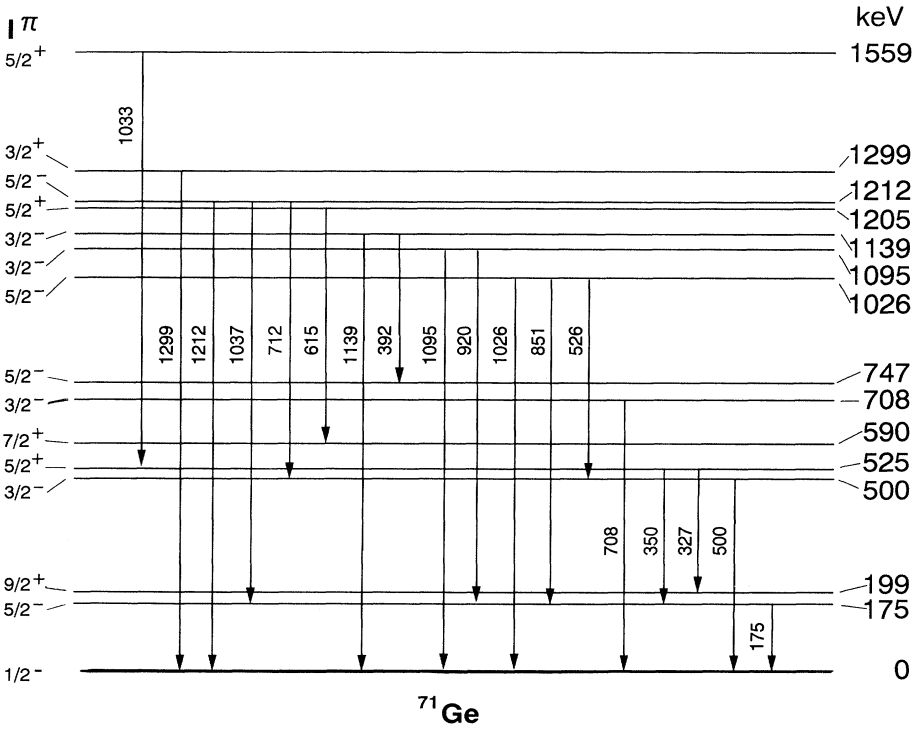

FIG. 1. A simplified level scheme of ^{71}Ge showing the transitions whose anisotropies were measured.

it is then possible to deduce other A_2 coefficients from a comparison of anisotropies. The mixing ratios deduced from the A_2U_2 values are given in Table II and possible δ values are not unique in most cases. Several of the transitions deserve special mention and this is done in order of decreasing level energy. Their place in the decay scheme is indicated in Fig. 1.

The 1559-keV $\frac{5}{2}^+$ level. We assume that the first-forbidden β decay is $\Delta j_\beta=1$ and thus $U_2=0.657$. Any $\Delta j_\beta=2$ admixture will have the effect of increasing the A_2 coefficient and extend the range of the δ value.

The 1212-keV $\frac{5}{2}^-$ level. In the subsequent theoretical analysis this state is considered to be an intruder and no predictions are made for multipole mixing ratios. The large U_2A_2 coefficient of the 712-keV $\frac{5}{2}^-$-$\frac{3}{2}^-$ transition implies that U_2 must be large and for the purpose of analysis we assume $\Delta j_\beta=0$ with $U_2=1$.

The 1026-keV $\frac{5}{2}^-$ level. The anisotropy of the ground-state transition is consistent with a $\Delta j_\beta=0$ β decay although a $\Delta j_\beta=1$ contribution may be present. Any contribution would increase the δ value of the 526-keV $\frac{5}{2}^-$-$\frac{3}{2}^-$ transition from which the alternative second-order solution is excluded by the small fourth-order term; cf. Table I.

The 708-keV $\frac{3}{2}^-$ level. We cannot exclude an $I=\frac{1}{2}$ assignment. As there are several γ rays of unknown character feeding the level it is not possible to deduce the γ-ray multipole mixing ratio if the level spin is $\frac{3}{2}^-$.

The 525-keV $\frac{5}{2}^+$ level. Using the more precise value of Ref. [5] we obtain $U_2=0.811(47)$ for the feeding transitions. The decay scheme indicates that these are dominated by β decay and, consequently, there is a substantial $\Delta j_\beta=1$ component of 55(13)%. With this U_2 value we obtain A_2 for the 350-keV $\frac{5}{2}^+$-$\frac{5}{2}^-$ transition and hence $\delta=-0.19(3)$. This large $M2$ admixture implies a significant K forbiddness.

III. THEORETICAL ANALYSIS

The calculations reported in Ref. [1] have been extended to provide δ values that may be compared with the experimental results. Previous theoretical investigations of ^{71}Ge [8] were in the framework of the particle-vibration model [9] and, together with ^{69}Ge, in the cluster-vibration model [10] in which one and three particles in the $N=28$–40 subshell were respectively, coupled to quadrupole vibrations.

The interacting boson-fermion model (IBFM) calculation reported in Ref. [1] was performed using a ^{70}Ge core and BCS neutron quasiparticles in accordance with Kisslinger-Sorensen parametrization [11]. The boson-fermion interaction strengths were adjusted to the energy spectrum of ^{71}Ge. To obtain the positive-parity states we have included, in addition to the $N=28$–50 valence shell configurations, the $d_{5/2}$ single-particle configuration from the shell above. The effective charges and gyromagnetic ratios were chosen in order to reproduce the experimental values for the static moments $\mu(\frac{1}{2}_1^-)$, $\mu(\frac{5}{2}_1^-)$, $\mu(\frac{9}{2}_1^+)$, and $Q(\frac{9}{2}_1^+)$ of levels in ^{71}Ge [15]. Employing this parametrization, the branching ratios were calculated and compared to the experimental data. We have now extended the calculation to the multipole mixing ratios given in Table II. The initial states for transitions investigated in the present experiment are assigned to the levels calculated in the IBFM; cf. Table II. In accordance with Ref. [1], the 1026-, 1095-, 1139-, and 1299-keV levels are assigned to the calculated negative-parity levels $\frac{5}{2}_3^-$, $\frac{3}{2}_4^-$, $\frac{3}{2}_5^-$, and $\frac{3}{2}_6^-$, respectively [Fig. 3(a) of Ref. [1]], and the 1205- and 1559-keV levels to the calculated $\frac{5}{2}_2^+$ and $\frac{5}{2}_3^+$ positive-parity levels, respectively [Fig. 3(b) of Ref. [1]]. The $\frac{5}{2}^-$ level at 1212 keV is associated with the intruder band [1] lying outside the scope of the IBFM valence-shell calculation.

As it may be seen from Table II, the absolute values of the calculated mixing ratios are in agreement with experiment. In the cases with two alternative experimental results, the calculated values favor one of the two possibilities. In addition, in Table III, we compare the available experimental values for reduced transition probabilities with the results of the present calculation.

In Ref. [8], it was argued that the presence of the low-lying $\frac{5}{2}^+$ state close to the $\frac{9}{2}_1^+$ level and the absence of a $\frac{13}{2}^+$ level near $\frac{9}{2}_1^+$ provide evidence that the positive-parity spectra of both ^{71}Ge and ^{69}Ge resemble the theoretical pattern arising from the cluster-vibration model, i.e., involve the seniority-three configuration in the unique-parity orbital $g_{9/2}$. In the IBFM calculation a similar effect is simulated by the exchange force [14], although the $g_{9/2}$ occupation probability is rather low. Particularly interesting for a theoretical interpretation is the decay pattern of the $\frac{5}{2}_2^+$ level. Experimentally, the strongest branch is to the $\frac{7}{2}_1^+$ level, with a multipole mixing ratio which reveals $M1$ dominance. This pattern is well reproduced by the IBFM calculation. If we consider only the sizable components (with amplitudes larger than 4%), the wave functions of the relevant group of positive-parity states can be approximately presented in block form:

$$|\tfrac{5}{2}_2^+\rangle \approx |g_{9/2},4_1^c;\tfrac{5}{2}\rangle ,$$

$$|\tfrac{9}{2}_1^+\rangle \approx |g_{9/2},0_1^c;\tfrac{9}{2}\rangle -0.4|g_{9/2},2_1^c;\tfrac{9}{2}\rangle ,$$

TABLE III. Experimental reduced transition probabilities and IBFM values.

$I_i\rightarrow I_f$	$B(E2)$ (e^2b^2) Expt.	IBFM	$B(M1)$ (μ_N^2) Expt.	IBFM
$\frac{5}{2}_1^-\rightarrow\frac{1}{2}_1^-$	0.0050(5)[a]	0.0001		
$\frac{9}{2}_1^-\rightarrow\frac{5}{2}_1^-$	0.015(4)[b]	0.0063		
$\frac{11}{2}_1^+\rightarrow\frac{9}{2}_1^+$	0.034(12)[b]	0.0200	0.021(7)[b]	0.0321
$\frac{13}{2}_1^+\rightarrow\frac{9}{2}_1^+$	0.075(15)[b]	0.0420		
$\frac{11}{2}_2^+\rightarrow\frac{7}{2}_1^+$	0.095(22)[b]	0.0155		
$\frac{11}{2}_2^+\rightarrow\frac{9}{2}_1^+$	0.015(4)[b]	0.0008	0.0010(5)[b]	0.0012

[a]Reference [12].
[b]Reference [13].

$$|\tfrac{5}{2}_1^+\rangle \approx |g_{9/2}, 2_1^c; \tfrac{5}{2}\rangle ,$$

$$|\tfrac{7}{2}_1^+\rangle \approx |g_{9/2}, 2_1^c; \tfrac{7}{2}\rangle - 0.4|g_{9/2}, 4_1^c; \tfrac{7}{2}\rangle .$$

Here 0_1^c, 2_1^c, and 4_1^c denote the IBM wave functions of the positive-parity core states 0_1, 2_1, and 4_1, respectively. In this approximate classification, the $M1$ matrix element is allowed for the $\frac{5}{2}_2 \rightarrow \frac{7}{2}_1$ transition and the $E2$ matrix element for the $\frac{5}{2}_2^+ \rightarrow \frac{7}{2}_1^+$ and $\frac{5}{2} \rightarrow \frac{5}{2}_1^+$ transitions. The corresponding IBFM values, $B(M1; \frac{5}{2}_2^+ \rightarrow \frac{7}{2}_1^+) = 0.29\mu_N^2$, $B(E2; \frac{5}{2}_2^+ \rightarrow \frac{7}{2}_1^+) = 0.022\ e^2b^2$, and $B(E2; \frac{5}{2}_2^+ \rightarrow \frac{5}{2}_1^+) = 0.026\ e^2b^2$, give $I_\gamma(\frac{5}{2}_2^+ \rightarrow \frac{7}{2}_1^+)/I_\gamma(\frac{5}{2}_2^+ \rightarrow \frac{5}{2}_1^+) = 100/18$, in rather good agreement with the experimental ratio 100/7. The calculated value of the $\frac{5}{2}_2^+ \rightarrow \frac{7}{2}_1^+$ mixing ratio, $\delta = -0.14$, is also in good agreement with the magnitude and sign of the measured value $\delta = -0.23^{+0.09}_{-0.08}$.

We note that the IBFM calculation gives a specific pattern for depopulation of $\frac{3}{2}^-$ levels: The reduced transition probabilities for depopulation of the $\frac{3}{2}_4^-$ level are significantly smaller than for depopulation of the $\frac{3}{2}_5^-$ and $\frac{3}{2}_6^-$ levels. Accordingly, the calculated half-life of the $\frac{3}{2}_4^-$ level is much longer than those of $\frac{3}{2}_5^-$ and $\frac{3}{2}_6^-$ levels.

The only transition in Table II with both large $B(E2)$ and $B(M1)$ values is $\frac{5}{2}_2^+ \rightarrow \frac{7}{2}_1^+$ and therefore in this case the signs of calculated matrix elements are reliable; both the sign and magnitude of the calculated mixing ratio are in agreement with the smaller experimental value. The only remaining case with a sizable $B(M1)$ value is $\frac{3}{2}_5^- \rightarrow \frac{5}{2}_2^-$ and in this case the $M1$ component dominates over $E2$.

In five of the results the agreement between a measured and calculated δ value is close despite the limitations of the model calculations for a quantity that can vary between $+\infty$ and $-\infty$ and that is also sensitive to model details. For several of the remaining transitions in Table II the calculated signs of the multipole mixing ratio differ from the ones deduced from experiment, while the calculated magnitudes are in qualitative agreement with the experiment. This might be attributed to the fact that in these cases one or both transition matrix elements are very small and thus, due to interference among small terms, the signs of the transition amplitudes might not be reliable. In general, the IBFM calculations give a rather good description of the experimental features of ^{71}Ge.

ACKNOWLEDGMENTS

We are indebted to Breese Quinn who analyzed foil stacks in preliminary experiments. W.L.C. and W.H.B. acknowledge the support of ORAU and W.D.H. that of the Joint Institute for Heavy Ion Research and Vanderbilt University. UNISOR is a consortium of universities, the State of Tennessee, Oak Ridge Associated Universities, and Oak Ridge National Laboratory and is partially supported by them and by the U.S. Department of Energy under Contract No. DE-AC05-76OR00033.

[1] R. A. Meyer, R. J. Nagle, S. Brant, E. Frlež, V. Paar, and P. K. Hopke, Phys. Rev. C **41**, 686 (1990).
[2] F. Iachello and O. Scholten, Phys. Rev. Lett. **43**, 679 (1979).
[3] A. Arima and F. Iachello, Ann. Phys. (N.Y.) **99**, 253 (1976).
[4] V. Paar, S. Brant, L. F. Canto, G. Leander, and M. Vouk, Nucl. Phys. **A378**, 41 (1982).
[5] D. I. Bradley, Hyperfine Interact. **35**, 1033 (1987).
[6] R. M. Steffen and K. Alder, in *The Electromagnetic Interaction in Nuclear Spectroscopy,* edited by W. D. Hamilton (North-Holland, Amsterdam, 1975).
[7] D. C. Camp and A. L. van Lehn, Nucl. Instrum. Methods **76**, 192 (1969).
[8] V. Paar, U. Eberth, and J. Eberth, Phys. Rev. C **13**, 2532 (1976).
[9] A. Bohr and B. R. Mottelson, K. Dan. Vidensk. Selsk. Mat. Fys. Medd. **27**, No. 16 (1953).
[10] V. Paar, Nucl. Phys. **A211**, 29 (1973).
[11] L. S. Kisslinger and R. A. Sorensen, Rev. Mod. Phys. **35**, 853 (1963).
[12] G. Murray, N. E. Sanderson, and J. C. Willmot, Nucl. Phys. **A171**, 435 (1971).
[13] U. Eberth, J. Eberth, E. Eube, and V. Zobel, Nucl. Phys. **A257**, 285 (1976).
[14] O. Scholten, Ph.D. thesis, University of Groningen, 1980.
[15] P. Raghavan, At. Data Nucl. Data Tables **42**, 189 (1989).